TASK ALLOCATION AND STOP OPTIMIZATION FOR AUTONOMOUS WEEDING

DAVID RAZHIEL CERES ARROYO

A Multi-Tool Allocation Approach for Optimized Weed Removal in Autonomous Agriculture

June 2025 – classicthesis v4.8

ABSTRACT

Short summary of the contents in English. . . a great guide by Kent Beck how to write good abstracts can be found here:

https://plg.uwaterloo.ca/~migod/research/beckOOPSLA.html

ZUSAMMENFASSUNG

Kurze Zusammenfassung des Inhaltes in deutscher Sprache. . .

We have seen that computer programming is an art,
because it applies accumulated knowledge to the world,
because it requires skill and ingenuity, and especially
because it produces objects of beauty.

— Donald E. Knuth [6]

ACKNOWLEDGMENTS

Put your acknowledgments here.

Many thanks to everybody who already sent me a postcard!

Regarding the typography and other help, many thanks go to Marco Kuhlmann, Philipp Lehman, Lothar Schlesier, Jim Young, Lorenzo Pantieri and Enrico Gregorio, Jörg Sommer, Joachim Köstler, Daniel Gottschlag, Denis Aydin, Paride Legovini, Steffen Prochnow, Nicolas Repp, Hinrich Harms, Roland Winkler, Jörg Weber, Henri Menke, Claus Lahiri, Clemens Niederberger, Stefano Bragaglia, Jörn Hees, Scott Lowe, Dave Howcroft, José M. Alcaide, David Carlisle, Ulrike Fischer, Hugues de Lassus, Csaba Hajdu, Dave Howcroft, Anonymous, Konrad Höffner, and the whole LaTeX-community for support, ideas and some great software.

Regarding LyX: The LyX port was intially done by *Nicholas Mariette* in March 2009 and continued by *Ivo Pletikosić* in 2011. Thank you very much for your work and for the contributions to the original style.

CONTENTS

LIST OF FIGURES

LIST OF TABLES

LISTINGS

ACRONYMS

TA Task Allocation

SVCA Shapley Value Clustering Algorithm

CBDTA Consensus-Based Distributed Task Allocation Algorithm

VDKM Voronoi Diagram-Based, K-Means Algorithm

CBBA Consensus-Based Bundle Algorithm

CBPAEA Consensus Based Parallel Auction and Execution Algorithm

GRU Gated Recurrent Units

MLP Multi-Layer Perceptron

EDACAM Encoder Decoder Architecture with Cross Attention Mechanism

GNN Graph Neural Network

CNN Convolutional Neural Network

PSO Particle Swarm Optimization Algorithm

GTODT Group Theory and Optimization Duality Theory

MIQP Mixed-Integer Quadratic Program

GA Genetic Algorithm

COQP Constraint Optimization as Quadratic Program

DEMP Diferential Evolution for Multimodal Problems

IT Implement Tool

DOF Degrees of Freedom

URDF Unified Robot Description Format

SDF Simulation Description Format

WS Workspace

DFS Depth-First Search

BFS Breadth-First Search

MIP Mixed-Integer Programming

1

INTRODUCTION

1.1 BACKGROUND AND CONTEXT

Autonomous systems are complex agents capable of carrying out operations without human intervention. They have become more capable thanks to technological advancements and increasingly integrated into society with recent remarkable progress in artificial intelligence (AI) techniques. According to Zhang in [14], current trends indicate that the development and adoption of such systems will continue to grow in the coming years.

The agricultural sector is one of the areas where the integration of autonomous technologies has great potential. These systems could significantly benefit farmers by making their work safer and less repetitive. Autonomous systems have already been used in alternative cropping methods such as precision agriculture. Nevertheless, traditional practices are still facing challenges that autonomous systems could perfectly address. Among these challenges, the proliferation of weeds in grass fields raises as a major concern for the livestock well-being for two main reasons. First, weeds compete with grass for resources, reducing the quality of food available for grazing animals. Second, some weed species pose a direct threat to livestock health. In particular, plants like Rumex have been identified as toxic and the cause of livestock poisoning [11].

Removing these plants is a task that farmers must perform manually, as EU regulations restrict the use of pesticides and prevent farmers from combating weed proliferation through chemical means. It is evident that this task, especially in large grass fields, is highly time-consuming and extremely repetitive, making it an ideal candidate for automation. In Germany, companies like Paltech have developed solutions to address this problem using autonomous wheeled robots. Their flagship robot is a differential-drive wheeled system equipped with various sensors for localization and weed detection, as well as an onboard drilling mechanism for weed removal. Currently, if the weed removal process needs to be sped up, the only solution is to deploy a fleet of robots. While this is feasible, developing single units capable of holding more than one drilling mechanism seems like the natural next step in Paltech's solution.

1.2 PROBLEM STATEMENT

The development of systems with more than one drilling unit for weed removal comes with both hardware and software challenges. It is crucial to ensure that tools and system resources are used as efficiently as possible. We want to avoid having more capable units with unused tools, especially since the production and deployment of these improved systems are more costly. Therefore, reducing idle time is a top priority and the focus of this thesis.

Idle time refers to periods when resources, such as drilling equipment, are not actively engaged in productive work. Reducing idle time in this context means minimizing the time tools remain unused and maximizing their productivity in weed removal. To achieve this, allocating detected plants to the correct tools is essential. In the literature, this process is known as TA. Some technical challenges to consider during implementation include computational latency and multi-tool coordination. The TA algorithm and execution pipeline must be fast enough to process new detections and reassign tools in real time without causing delays, while also ensuring that multiple drilling units operate efficiently without interference or redundancy.

1.3 CURRENT SOLUTIONS

In general, a task allocation system aims to achieve an efficient assignment of tasks to robots (or tools in this case) by considering various characteristics such as the robots' capabilities, task requirements, and system efficiency. This process of task allocation involves three important factors to be consider acording to Umashankar in [4]. Robot/tool, environment and coordination as shown in Figure 1.1.

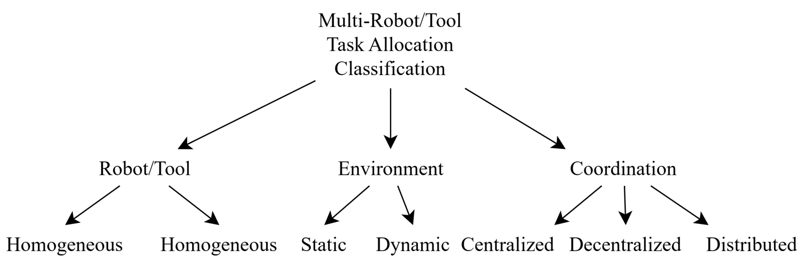

Figure 1.1: Multi-robot task allocation classification. Source [4]

An example of homogeneous tools in this context is a robot equipped with multiple tools of the same type, such as drills. In contrast, heterogeneous tools refer to robots equipped with different types of tools, such as drilling, seeding, and sensing equipment.

The multi-tool task allocation can take place in either a dynamic or static environment. In an environment that is static in nature, tasks are allocated to tools in advance before they begin to execute them. This method works well in situations when the tasks are predetermined and the environment remains unchanged. In contrast, dynamic task allocation involves the real-time assignment of tasks to tools as they carry out their activities. For the scope of this thesis, we will focus on homogeneous tools operating in a dynamic environment with centralized coordination, where the onboard computer will act as the master, assigning plants to each drilling mechanism.

There are several ways to accomplish multi-tool allocation, including heuristic, cluster-based, market-based, learning-based, and optimization-based techniques. Table 1.1 and 1.2 presents a comprehensive classification of task allocation algorithms found in the literature.

APPROACH	TECHNIQUE/ALGORITHM
Cluster Based	SVCA [10]
	Group Agent Partitioning [3]
	CBDTA [1]
	VDKM [5]
	CBBA [12]
	Cluster First Consensus-Based Strategy
	K-Means Clustering
Market Based	Auction Algorithm [7]
	Improved Auction Algorithm [13]
	Extended Auction Algorithm
	Distributed Auction Algorithm
	Sequential Single-Item Auctions
	Auction-Based Algorithm
	Multihop-Based auction Algorithm
	Based on Sequential Single Item Auctions
	CBPAEA
	Extended Sequential Single Item Auction
	Distributed Auction-Based Algorithm
	The Consensus-Based Bundle Algorithm
	Linear Integer Programming
	Contract Net Protocol

Table 1.1: Comparative overview of cluster-based and market-based approaches to multi-agent TA. [4]

In cluster-based approaches, the goal is to group tasks into a predefined number of clusters. Instead of assigning a single task to each tool, the clustering approach allocates entire groups of tasks to them, reducing the number of individual task assignments and computational

APPROACH	TECHNIQUE/ALGORITHM
Learning Based	GRU, MLP [9]
	Deep Reinforcement Learning [2]
	Heterogeneous Graph Attention Network
	Capsule Attention-Based Mechanism
	EDACAM
	Graph Neural Network (GNN)
	Q-Learning, CNN and a GRU
	Graph Convolutional Neural Networks
Optimization Based	Mixed-Integer Quadratic Program
	Centralized Hungarian Method [8]
	Bin Maximum Item Doubled Packing
	PSO
	GTODT
	Integer Programming
	MIQP
	Genetic Algorithm (GA), A* Algorithm
	COQP
	Heuristic Based
	DEMP
	Fuzzy Optimization

Table 1.2: Comparative overview of learning-based and optimization-based approaches to multi-agent TA. [4]

complexity. Clustering approaches aim to minimize travel distance and maximize task coverage by grouping tasks effectively. However, the optimal clustering of tasks still needs further exploration. Although these approaches simplify task allocation, they struggle to handle dynamic changes in the environment.

An optimization-based strategy aims to select the best solution from a set of available options. These solutions are constrained by specific conditions, and the optimal one is determined based on the objective function. The objective function represents the system's ultimate goal. Some of the optimization algorithms have poor robustness to uncertainties therefore this approach is more suitable for solving well-defined and static problems focusing on theoretically optimal or near-optimal solutions. Additionally, optimization-based approaches require more computational power and are less adaptable to changing environments.

Market-based approaches effectively handle highly combinatorial optimization problems. In this method, an auctioneer informs agents about available tasks and requests bids. Each agent evaluates its capacity to complete the tasks and submits a bid accordingly. The auctioneer then assigns tasks to the agent with the most favorable bid. Generally, task allocation using this approach minimizes travel time. While these methods are flexible and scalable, they may not always achieve a globally optimal solution.

Recent approaches to task allocation incorporate deep learning techniques such as graph neural networks and graph convolutional networks. These types of task allocation methods are commonly referred as learning-based approaches. Most learning-based approaches struggle to generalize to larger-scale problem scenarios beyond those used during training. This characteristic is especially important because real-world task allocation problems frequently require modeling scenarios whose costs increase with the number of tasks and robots. Table 1.3 gives a comparison between all the approaches.

	Clustering	**Optimization**	**Market-Based**	**Learning-Based**
Advantage	Simplifies task allocation and reduces complexity	Provides optimal solutions, well suited for static problems	Flexible, scalable, decentralized	Adaptable, learns, and improves over time
Limitation	May not account for dynamics well	Computationally intensive, less adaptable	May not yield global optima, and needs effective bidding	Requires training time, initially suboptimal
Best case	Logical tasks	Well-defined, static problems	Dynamic environments with varying tasks	Complex and uncertain environments
Future work	Dynamic clustering, online adaptation	Hybrid models, real-time optimization	Adaptive market mechanisms, incentive models	Transfer learning, meta-learning

Table 1.3: A Comparison of different approaches to TA, Source [4]

1.4 PROPOSED SOLUTION

As Table 1.3 illustrates, algorithm selection must be carefully considered based on the application's nature to achieve optimal performance. In a grass field clearing application, the environment is highly dynamic, especially since weed detections occur while the system is in motion. Therefore, market-based approaches are well-suited to ensuring the system adapts effectively to such conditions. However, since weeds often spread in clustered areas, a cluster-based approach could help reduce the algorithm's computational load and improve real-time responsiveness.

A hybrid algorithm is proposed to tackle the dynamics of the environment and leverage the benefits of both market-based and cluster-based approaches. By combining real-time adaptability with efficient task grouping, the system can dynamically allocate tasks while minimizing computational overhead. This approach ensures that weed removal remains efficient even as new detections occur, ultimately improving performance in large-scale and rapidly changing field conditions.

2

SIMULATION

2.1 THE ROBOT

Nuga is Paltech's solution for speeding up the weed removal process. Nuga is a mobile platform equipped with two drilling mechanisms, also called IT, one main camera at the front for plant detection, two internal cameras for fine adjustment during tools' placement, an IMU, and two GNSS antennas for GPS localization. Each IT is mounted on a structure with three Degrees of Freedom (DOF) using prismatic joints, allowing movement in X, Y, and Z directions.

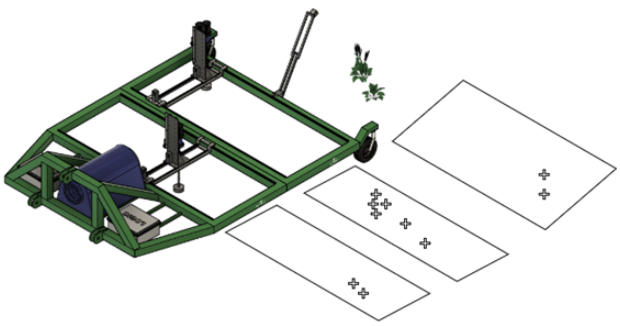

Figure 2.1: Nuga Platform

2.2 SIMULATION

A representative simulation of reality is crucial for developing new algorithms and analyzing robot behavior before real-world implementation. Therefore, building a simulation of the project was a foundational step for this work, ensuring a controlled environment for validation and testing. Gazebo[1] was the selected tool because it provides a physics engine, supports sensor and actuator modeling, and integrates well with ROS[2], making it ideal for testing robotic systems.

The simulation consists of six key components: URDF files define the robot's structure and properties, SDF files describe the virtual environment, and Gazebo plugins provide additional functionality, such as simulating custom sensors, actuators, or control interfaces.

1 Gazebo is a physics-based robotics simulation tool that allows testing and validation of robot models before real-world deployment. https://gazebosim.org/home

2 ROS (Robot Operating System) is an open-source framework that provides tools, libraries, and conventions for developing, managing, and simulating robotic applications. https://www.ros.org/

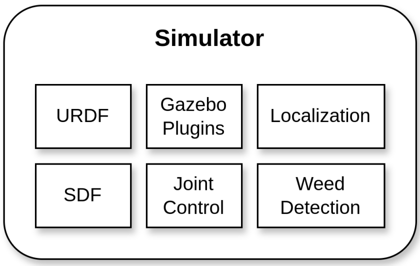

Figure 2.2: Simulator Components

Additionally, core system operations include joint control for managing the movement of the IT, localization for tracking the robot's position, and weed detection, which relies on an AI model for Rumex recognition. Figure 2.2 illustrates these components as building blocks for the simulation.

2.2.1 *URDF*

Unified Robot Description Format (URDF) is an XML file used to describe multibody systems for robot simulation. It defines the visual, collision, and inertial properties of rigid body objects, as well as their connections (*joints*). This establishes a spatial relationship between frames, which ROS and Gazebo can later interpret for control and visualization. This file also allows modeling different types of sensors and incorporating Gazebo plugins to link it with ROS control actions. We exploit these capabilities to define camera intrinsics, IMU behavior, GPS properties, and control the IT using `ros2_control`[3].

Figure 2.3a displays the structure of the URDF files, being nuga the highest level entity that joins the robot description, gazebo sensor modeling and plugins, as well as `ros2_control` configuration. Nuga description defines the robot's physical structure, including its links (e.g., chassis, wheels, camera support), joints (fixed, continuous, prismatic connections), sensors (cameras, IMU, GPS), and inertial properties. It organizes these components into a kinematic tree (e.g., base_link -> chassis_link -> wheels/sensors) using macros for modularity, and resulting in the model displayed in Figure 2.3b.

2.2.2 *SDF*

Simulation Description Format (SDF) also written in XML, describes the properties of the virtual world. Gazebo uses this file to define the terrain, obstacles, lighting conditions, physics parameters, and other

3 `ros2_control` is a ROS 2 framework that provides a standardized interface for managing hardware, enabling modular and reusable control systems for robots. https://control.ros.org/rolling/doc/getting_started/getting_started.html

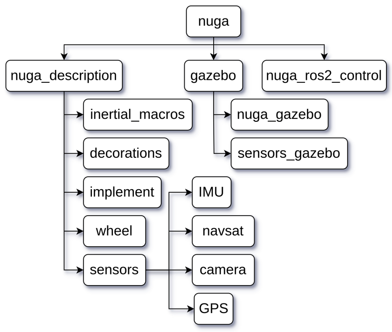

(a) URDF files structure.

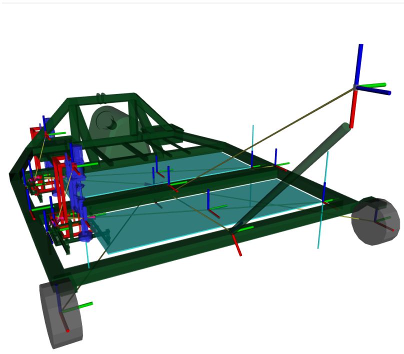

(b) RViz visualization of Nuga description.

Figure 2.3: Robot definition using URDF

environmental elements that affect the robot's interaction with the simulation. Having repeatability in a simulated world is important for debuging and testing purposes, for this reason a Python script was used to generate easy to configure worlds from a YAML configuration file. An example of the config file is shown in Listing A.1. For reproducibility, a seed value is configured in the simulation settings, the weed infestation pattern is defined within quadrants of specified dimensions (`quadrant_size`) and each quadrant is individually configured with:

- Spatial distribution:
  - *uniform*: Random uniform distribution
  - *clustered*: Random normal distribution with definable standard deviations (σ_x, σ_y)
- Weed density: Weeds per square meter (weeds/m^2)
- Direction: Propagation axis for adjacent quadrants $(\pm x, \pm y)$
- Workspace expansion: If `outside_workspace` is true, the infestation area extends 10% beyond the quadrant boundaries.

A visual result of the generated world using such configuration file is shown in Figure 2.4.

2.2.3 *Gazebo Plugins*

The files `nuga_gazebo` and `sensors_gazebo` from Figure 2.3a instantiate and configure Gazebo plugins to define sensor behavior, including optical properties for the camera, as well as update rates and noise models for the IMU and GPS. The file `nuga_ros2_control` on the other hand, establishes an interface between the IT 's joints and

Figure 2.4: Weed Infestation Example

ros2_control framework, specifying the command interface (position), controller type (forward position controller), and movement limits, enabling 3-DOF prismatic motion for each tool. Regarding movement control of the Nuga vehicle, the ros_planar_move plugin satisfied all control requirements given the platform's kinematic constraints, eliminating the need for additional configuration.

2.2.4 *Joint Control*

The control of both IT units was handled using the ros2_control framework (configuration example shown in Listing A.2), as previously described. This framework provides a seamless transition between simulation and real hardware control. In this context, the forward_command_controller was used, which is recommended for simulation because it bypasses PID computations by directly sending commands to simulated joints. These joints already track positions perfectly, without the disturbances or error correction needed in real-world scenarios. Simulators like Gazebo inherently handle ideal position tracking, making closed-loop control redundant. However, when switching to real hardware, replacing it with a position_controller is needed but straightforward thanks to the flexibility of the framework.

Nuga's workspace layout and dimensions are shown in Figure 2.5. The gantry carrying the IT operates within a zone of 2.09 m in the Y direction, 0.72 m in X, and 0.26 m in Z. An extraction cycle begins with the gantry moving in X and Y to position the tool above the plant, followed by a downward movement in Z to lower the drill and perform the extraction. The gantry has a maximum speed of $1\frac{m}{s}$ in the XY plane, and each extraction can take up to 45 seconds per plant.

The IT is controlled using ROS2 actions, which provide a structured way to handle asynchronous tasks with feedback and result reporting. For the XY movement of the gantry, the AxisPosition action is used, allowing the specification of target coordinates (x, y) and speed, while providing feedback on the current position and confirming whether

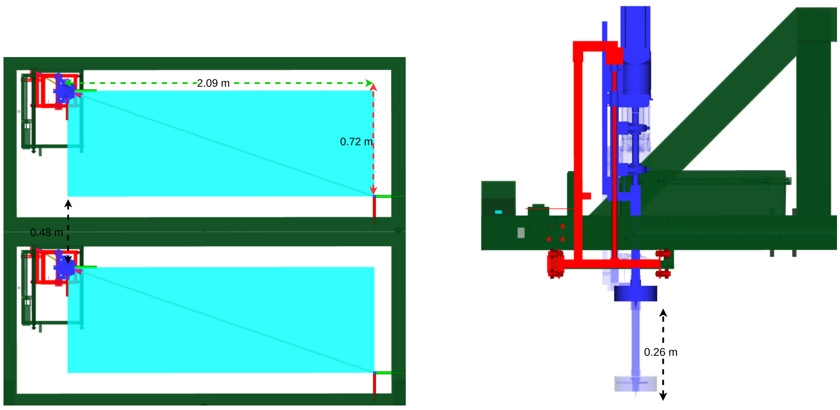

(a) X, Y Workspace (b) Z Workspace

Figure 2.5: IT Workspace Layout

the target was reached. The `Extraction` action manages the vertical movement of the tool along the Z axis, reporting the depth reached, total time taken, and success status, along with real-time feedback on the current depth. Finally, the `ExtractionCycle` action coordinates the execution of multiple extractions by accepting an array of target poses and their corresponding IDs, providing feedback on the current status and reporting the results of the extraction process for each pose. These actions enable precise and modular control of the gantry system, ensuring efficient and reliable operation. A diagram summarizing this process is shown in Figure 2.6.

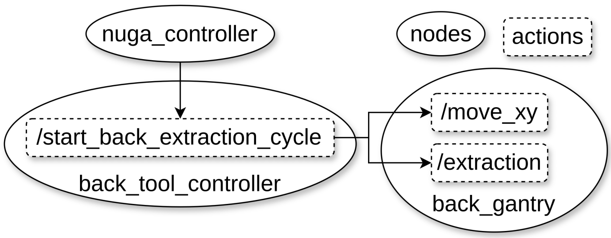

Figure 2.6: ROS Interface for back gantry control

2.2.5 *Localization*

Lorem ipsum dolor sit amet, consectetuer adipiscing elit. Ut purus elit, vestibulum ut, placerat ac, adipiscing vitae, felis. Curabitur dictum gravida mauris. Nam arcu libero, nonummy eget, consectetuer id, vulputate a, magna. Donec vehicula augue eu neque. Pellentesque habitant morbi tristique senectus et netus et malesuada fames ac turpis egestas. Mauris ut leo. Cras viverra metus rhoncus sem. Nulla et lectus vestibulum urna fringilla ultrices. Phasellus eu tellus sit amet tortor gravida placerat. Integer sapien est, iaculis in, pretium quis, viverra ac, nunc. Praesent eget sem vel leo ultrices bibendum. Aenean faucibus. Morbi dolor nulla, malesuada eu, pulvinar at, mollis ac, nulla. Curabitur auctor semper nulla. Donec varius orci eget risus. Duis nibh mi, congue eu, accumsan eleifend, sagittis quis, diam. Duis eget orci sit amet orci dignissim rutrum.

2.2.6 *Weed Detection*

Lorem ipsum dolor sit amet, consectetuer adipiscing elit. Ut purus elit, vestibulum ut, placerat ac, adipiscing vitae, felis. Curabitur dictum gravida mauris. Nam arcu libero, nonummy eget, consectetuer id, vulputate a, magna. Donec vehicula augue eu neque. Pellentesque habitant morbi tristique senectus et netus et malesuada fames ac turpis egestas. Mauris ut leo. Cras viverra metus rhoncus sem. Nulla et lectus vestibulum urna fringilla ultrices. Phasellus eu tellus sit amet tortor gravida placerat. Integer sapien est, iaculis in, pretium quis, viverra ac, nunc. Praesent eget sem vel leo ultrices bibendum. Aenean faucibus. Morbi dolor nulla, malesuada eu, pulvinar at, mollis ac, nulla. Curabitur auctor semper nulla. Donec varius orci eget risus. Duis nibh mi, congue eu, accumsan eleifend, sagittis quis, diam. Duis eget orci sit amet orci dignissim rutrum.

2.2.7 *Nuga Controller*

Lorem ipsum dolor sit amet, consectetuer adipiscing elit. Ut purus elit, vestibulum ut, placerat ac, adipiscing vitae, felis. Curabitur dictum gravida mauris. Nam arcu libero, nonummy eget, consectetuer id, vulputate a, magna. Donec vehicula augue eu neque. Pellentesque habitant morbi tristique senectus et netus et malesuada fames ac turpis egestas. Mauris ut leo. Cras viverra metus rhoncus sem. Nulla et lectus vestibulum urna fringilla ultrices. Phasellus eu tellus sit amet tortor gravida placerat. Integer sapien est, iaculis in, pretium quis, viverra ac, nunc. Praesent eget sem vel leo ultrices bibendum. Aenean faucibus. Morbi dolor nulla, malesuada eu, pulvinar at, mollis ac, nulla. Curabitur auctor semper nulla. Donec varius orci eget risus. Duis nibh mi, congue eu, accumsan eleifend, sagittis quis, diam. Duis eget orci sit amet orci dignissim rutrum.

3 TASK ALLOCATION AND OPTIMIZATION

Solving the TA problem in this context means assigning weed detections to removal tools in the most efficient way. The idea is to find the best allocation of resources and the optimal sequence of stops, that will maximize the number of plants removed, and minimize the tools' idle time. The solution has to consider the constraints of the problem such as:

GEOMETRIC CONSTRAINTS: A stop is considered valid only if the weeds lie within the workspaces of the tools (observe Figure 3.1).

MOVEMENT CONSTRAINTS: The robot can only move forward in a straight line at a max speed of $0.3\frac{m}{s}$.

TASK PROCESSING: Each plant removal takes approximately 45 seconds, during which the robot must remain stationary to ensure a successful extraction. Movement during this process is not allowed as it could compromise the tool operation.

DYNAMIC ENVIRONMENT: Weed positions are initially unknown and are discovered dynamically during operation by the camera in front of the vehicle.

PROCESSING TIME: The solution must run online because the robot discovers new weeds during operation, and decisions about stopping and TA must adapt in real-time.

We define a '*good*' stop as the next robot position that maximizes plant coverage while keeps a balance on the number of tasks assigned to each implement (aiming to minimize idle time). The problem can be approached in two ways: one option is to first determine the optimal stop location, after which task allocation becomes trivial by simply assigning tasks based on whether they fall within the front or back workspace. Alternatively, we can first allocate tasks to the implements and then compute the stop position that satisfies the corresponding geometric constraints. Both approaches are similar, differing mainly in the order of operations, but each perspective opens the door to different methods and algorithms to try.

3.1 METRICS

Defining a good set of metrics is crucial to establish a solid basis for comparison between solutions and to easily identify the flaws of

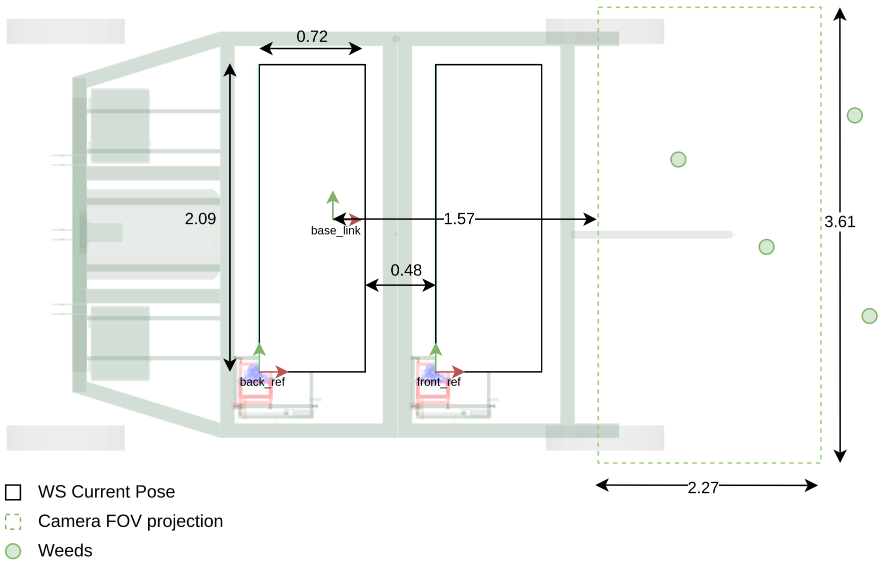

Figure 3.1: Problem Layout Dimentions

each method, thereby determining the best solution. To address this, we define two main categories. The first summarizes mission-level metrics such as the total idle and productive time of each tool, and the total time the robot spends moving or in a stationary state (defined by equations 3.1 and 3.2). The second category includes task-specific information, for example, task ID, status (*'compleated'*, *'failed'*, *'out'*), number of stops, the tool that processed the task, and the idle and productive time of each tool at that specific stop. These metrics are displayed in a mission dashboard for easy visualization and comparison across missions using different scenarios or algorithms (see Figure 3.2b for the first category and 3.2a for the second one).

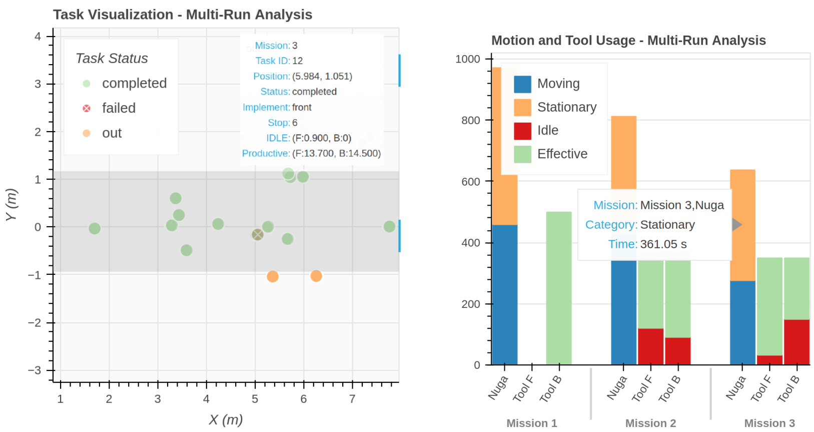

(a) Task Visualization (b) Mission Category Metrics

Figure 3.2: Mission Dashboard

FIGURE 3.2A Displays a 2D grid of the removed tasks' positions during the mission, along with their corresponding metadata. Hovering over a task reveals its details, and tasks can be filtered by mission.

FIGURE 3.2B Showcases a bar graph comparing different missions. Each mission includes the robot's moving and stationary time, as well as the idle and productive time of the onboard implement tools. A hover feature displays the value of each category.

$$t_{mission} = t_{moving} + t_{stationary} \tag{3.1}$$

$$t_{tool\_operation} = t_{idle} + t_{productive} \tag{3.2}$$

3.2 HEURISTICS

Heuristic solutions are commonly employed when the solution space of an optimization problem is too large to explore exhaustively, making an exact optimal solution computationally infeasible. They are also useful in time-sensitive scenarios, such as online implementations, where sacrificing optimality for efficiency is often justified.

In our work, we developed a heuristic algorithm to serve as a baseline solution, this provides a meaningful reference point to assess the performance and potential improvements offered by other algorithms. The algorithm' description is detailed in 1, with an illustrative example in Figure 3.3.

Algorithm 1 Heuristic

1: Get the position of the closest weed from the current robot position.

2: Project the tools' Workspace (WS) forward (in the future), aligning the trailing edge of the last WS with the closest weed's position plus a small clearance (e.g., 10 cm).
3: Allocate weeds to each tool if they fall within its projected WS.
4: Move the robot until the tools' WS are aligned with their projections, then execute the extractions for tools with assigned weeds.

5: Repeat the process until mission has ended.

This approach offers a simple implementation and fast computation solution, making it well-suited for online applications. However, its heuristic nature leads to suboptimal solutions, as it does not account for minimizing idle time. In Figure 3.4 we exemplify the algorithm' suboptimality for a particular case, contrasting with a better solution to support our analysis.

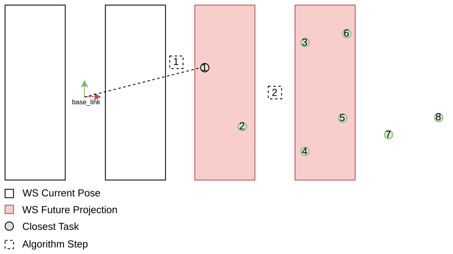

(a) S1.Closest task, S2.WS projection

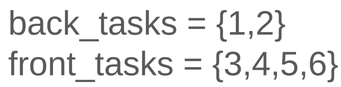

(b) S3.Task Allocation

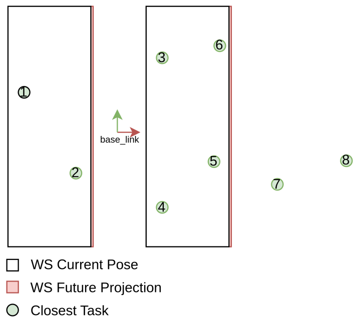

(c) S4.Moving until aligned and extraction

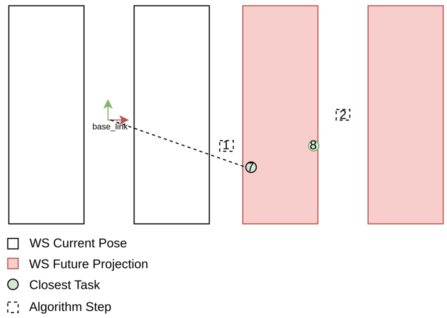

(d) S5.Repeat

Figure 3.3: Heuristic Algorithm

Figure 3.4a Showcases the two stops required to remove eight weed' detections, with the first stop allocating four tasks to the back tool and the second stop allocating two tasks to the front tool.

Figure 3.4b Illustrates the idle and productive time for the given solution. Blue represents the robot's repositioning time, red indicates the idle time of the respective tool, and white the productive time. The first stop shows a significant idle time for the front tool (90 seconds, equivalent to two tasks), caused by the tool waiting for the back tool to finish before proceeding to the next stop. The second stop shows a similar situation, where idle time arises from the only feasible option at that point: removing tasks 5 and 6 with the back tool.

An alternative solution for the same scenario (this time aimed at reducing idle time) is illustrated in Figure 3.5. In this case, the solution requires three stops: first stop assigns tasks 1 to back tool and task 5 to the front, the second stop processes tasks 2 and 6, and finally the third stop is used to remove tasks 3, 4, 7, and 8. As shown in Figure 3.5b, the balanced task allocation between tools eliminates idle time and reduces the total mission duration compared to the previous solution.

This demostrates the heuristic's suboptimality, as it fails to minimize idle time and does not consider the possibility of stopping at a location that allows for a more efficient task allocation. The heuristic algorithm is limited to the closest weed detection, which may not always be the best option. In the following sections, we will explore more sofisticated

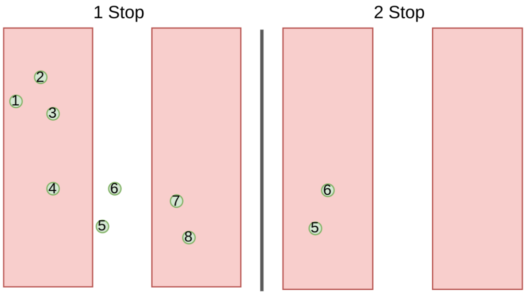

(a) Two stops required

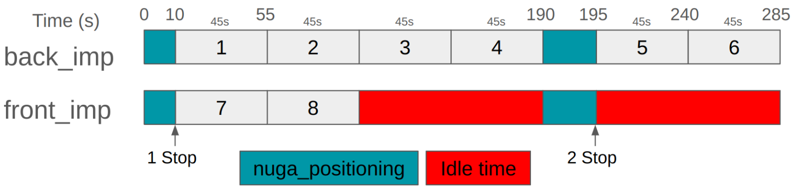

(b) Idle and productive time of each tool

Figure 3.4: Suboptimal solution computed using Heuristic

algorithms that can overcome these limitations and provide better solutions.

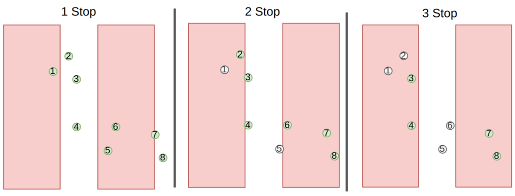

(a) Three stops required

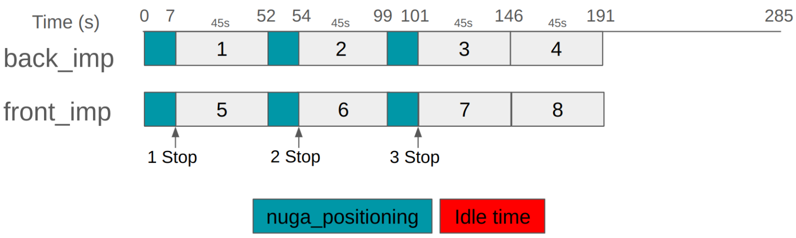

(b) Idle and productive time of each tool

Figure 3.5: Optimal solution

3.3 GRAPH SEARCH

Graph Search are a type of algorithms widely used in graph theory to systematically explore or traverse a graph. They are commonly used to find the shortest path between nodes, identify connected components, or solve various optimization problems. Graph search algorithms can be broadly categorized into two main types: uninformed and informed search algorithms.

Uninformed search algorithms do not have any additional information about the problem domain and explore the graph blindly. Examples include Depth-First Search (DFS) and Breadth-First Search (BFS). These algorithms are typically used for tasks like finding connected components or traversing all nodes in a graph. Informed search algorithms, on the other hand, use heuristics or additional information to guide the search process. They are often more efficient than uninformed algorithms for specific problems. Examples include A* search and Dijkstra's algorithm, which are commonly used for finding the shortest path in weighted graphs.

In our context, we exploit the advantages of graph-based algorithms by modeling the problem as such. Nodes represent potential stop locations, where two types of actions are possible: moving to another stop (a *stop node*) or performing weed removal at that location (an *action node*). Edge weights are defined as follows: edges between two *stop nodes* represent *travel cost*, computed using the distance between stops and the robot's velocity or a unitary value as a placeholder. Edges connecting a *stop node* to an *action node* represent *task execution cost*, and it is calculated based on the idle time (if any) of removing the indicated weeds with the assigned tools.

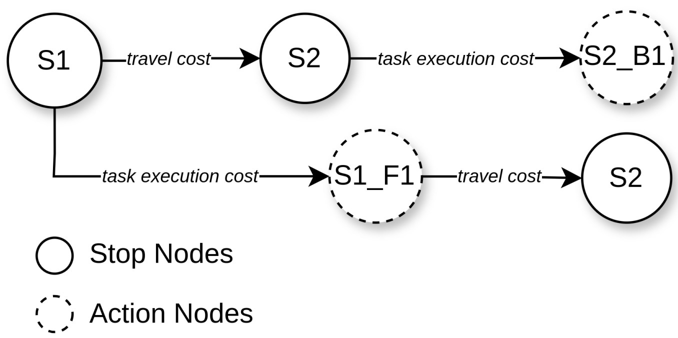

Figure 3.6: Node types and cost representation

FIGURE 3.6 Illustrates the convention used to represent the graph. `S1` denotes stop number 1, while `F` or `B` indicate whether the front or back tool is assigned to remove the weed, followed by the weed ID to be processed. In this example, the task execution cost between `S1` and `S1_F1` would be 45s, as the back tool must wait for the front tool to process 1 plant. The same logic applies to the cost between `S2` and `S2_B1` but for the front tool.

The graph search implementation solution follows the next pipeline:

1. Compute **candidate stops** based on the robot's current position and weed detections. Candidate stops are the locations where

an important event ocurs, such as a weed entering or exiting the workspace of a tool.

2. **Associate** reachable weeds with candidate stops. This allows the algorithm to determine which weeds can be removed at each stop.

3. Create a **graph representation** of the problem using DFS algorithm and the convention described in Figure 3.6. The graph is built by connecting *stop nodes* and *action nodes* using appropriate edge costs, taking into account the predefined associations between stops and tasks.

4. Get the **shortest path** in the graph from the root (first stop) to the final node (last stop) using Dijkstra's algorithm.

5. **Decode solution** and return the next optimal stop and task allocation as the algorithm's output.

To build and explore the graph, an implementation of the DFS algorithm is used (see Algorithm 4). The `get_children_nodes` method expands the graph by generating child nodes from a given parent node. If the parent node is a *stop node*, it creates child nodes for all valid combinations of reachable tasks that can be processed at that stop. Each combination forms a new child node that reflects the state after removing those tasks (*action node*). Additionally a 'trivial' *stop node* is addded representing the decision to move to the next stop without removing any weeds. On the other hand, if the parent node is an *action node*, this method creates a single *stop node* representing the next stop. Each created edge is added to the graph with a weight based on the associated *task execution cost* or *travel cost*. Figure 3.7 illustrates the graph expansion process, where the algorithm grows all possible combinations of tasks at each stop and generates the corresponding child nodes.

We observe that from `S3` four possible states can be reached (three *action nodes* and one *stop node*), The transition `S3_B1_F2` achieves zero idle time by optimally balancing tasks between the front and back tools, whereas the other transitions result in higher idle times due to imbalanced assignments. It's important to note that the same stop can be reached through different paths, depending on the actions taken at previous stops. For instance, if task 1 has been removed earlier, it should no longer be considered in subsequent stops. This consideration is crucial when building the graph, as we must ensure that it is expanded only through valid and realistic transitions that reflect feasible execution scenarios.

Having the complete graph, and given its configuration as a weighted directed graph, we choose Dijkstra's algorithm to find the optimal path (see Algorihtm 5). This algorithm efficiently explores the graph by maintaining a priority queue of nodes to be processed, ensuring that

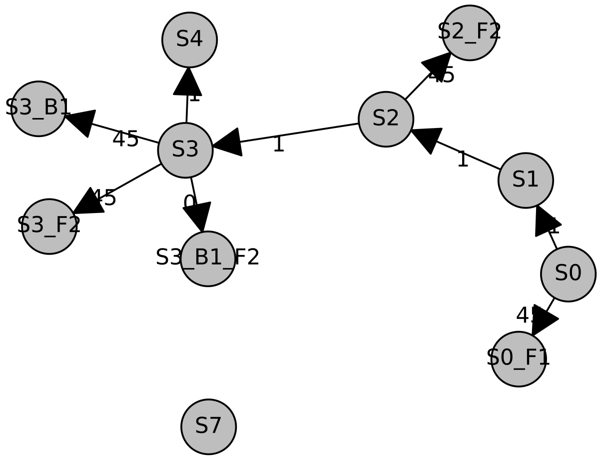

Figure 3.7: Graph expansion process

the node with the lowest cost is always explored first. The algorithm continues until it reaches the final node, which represents the optimal solution. The path is then traced back from the final node to the root, revealing the sequence of stops and actions that lead to the optimal solution.

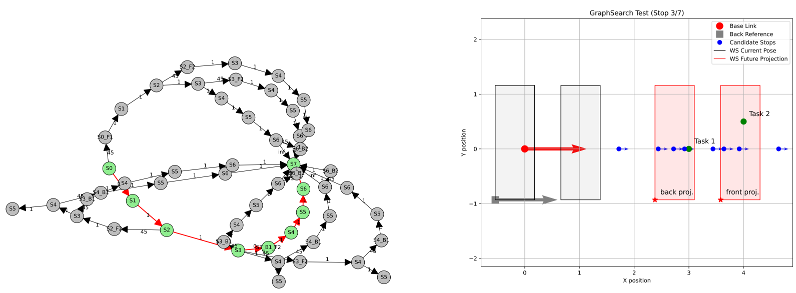

(a) Path with lowest cost

(b) Task Planning Visualization

Figure 3.8: Graph Search Solution

An optimal solution obtained by the graph search algorithm in a scenario with two detected weeds is illustrated in Figure 3.8a. The highlighted branch corresponds to the optimal path found by the algorithm. For the given two weeds, the graph contained 54 nodes, and the computation time was 0.001 seconds. A visual representation of the solution is shown in Figure 3.8b, including the current robot pose, projected workspaces in red, candidate stops in blue, and weeds in green.

One remaining issue to address is preventing the algorithm from returning trivial solutions in which either no weeds are removed or not all of them are. To tackle this, each node keeps track of the tasks completed so far. If, at the second-to-last node, there are still tasks left to remove, we assign a penalty cost to the edge leading to the final node. This encourages the algorithm to prioritize removing as many weeds as possible before proceeding to the last stop.

Our graph search solution performs well in terms of computation time, for a low to medium density of weeds. However, as the number of weeds increases, the graph size grows exponentially, leading to longer computation times. Figure 3.9 showcases the graph size and computation time for different number of weeds (see plot in red). The graph size is defined as the number of nodes in the graph, while the computation time is the time required to build and find the optimal path in the graph.

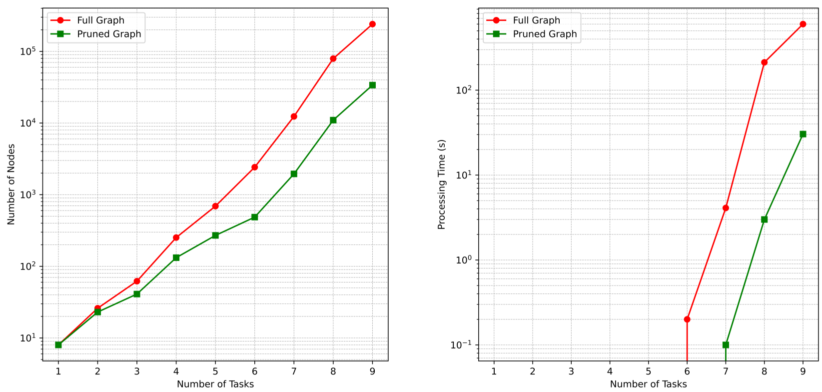

(a) Graph size vs. number of weeds

(b) Processing time vs. number of weeds

Figure 3.9: Graph Search algorithm performance

We were able to optimize and reduce the graph size by applying a pruning technique that stops the growth of certain branches when they are not promising. This is achieved by introducing the concept of *expired tasks*, these are tasks that haven't been removed and can no longer be removed in future stops because the corresponding weeds have been left behind, outside the tool's workspaces. This pruning is implemented in the `get_children_nodes` method, where each task is checked for expiration before being added to the graph. As a result, the number of nodes is significantly reduced, improving computation time (observe green plot in Figure 3.9).

Although the graph search algorithm is a promising approach, it still suffers from the exponential growth of the graph size as the number of weeds increases. This can lead to longer computation times and may not be suitable for real-time applications with high weed densities. In the next section, we will explore optimization-based approaches that can potentially overcome these limitations and provide more efficient solutions.

3.4 OPTIMIZATION

As discussed at the beginning of this chapter, the main goal of TA is to find the best allocation of resources and the optimal sequence of stops while considering the given constraints. Achieving such a solution requires mathematically formulating the scenario as an optimization task, with a clearly defined objective function, set of constraints, and decision variables that fully describe the problem. Optimization-based approaches are powerful tools that provide a systematic way to find the best feasible solution to a problem by exproring the solution space. Depending on the nature of the problem, a different optimization formulation can be used, such as linear programming, Mixed-Integer Programming (MIP), or nonlinear programming. In our case, we will focus on MIP as the most suitable approach for the problem.

MIP is a mathematical optimization technique that combines both integer and continuous variables in the formulation of the problem. It allows for the modeling of complex decision-making scenarios where some variables must take on discrete values (e.g., binary decisions) while others can take on continuous values. This flexibility makes MIP particularly useful for problems that involve resource allocation, scheduling, and other combinatorial optimization tasks.

Given a set of tasks $\mathcal{T} = \{1, 2, ..., T\}$ where each task $j \in \mathcal{T}$ corresponds to one weed detection from a total T, and a set of candidate stops $\mathcal{S} = \{1, 2, ..., S\}$ where each stop $i \in \mathcal{S}$ is computed using events as in Graph Search algorithm. Let $x_{i,j} \in \{0, 1\}$ be a binary decision variable equal to 1 if task j is assigned to stop i, 0 otherwise and $imb_i \in \mathbb{N}_0$ the imbalance of assigned tasks between tools at stop i. We know that from each stop i we can only assign tasks that are visible from that stop, and a subset for those corresponds to tasks set to front or back tools, these statements could be better defined as:

$\mathcal{V}_i \subseteq \mathcal{T}$	Set of tasks visible from stop i
$\mathcal{F}_i \subseteq \mathcal{V}_i$	Front tool task assigned at stop i
$\mathcal{B}_i \subseteq \mathcal{V}_i$	Back tool task assigned at stop i
τ	Constant processing time per task

We know that each task must be assigned to exactly one stop.

$$\sum_{i=1}^{S} x_{i,j} = 1 \quad \forall j \in \mathcal{T} \tag{3.3}$$

While visible tasks can only be assigned its corresponding stops.

$$x_{i,j} = 0 \quad \text{if} \quad j \notin \mathcal{V}_i \tag{3.4}$$

The imbalance per stop is the absolute time difference between front and back tools.

$$f_i = \sum_{j \in \mathcal{F}_i} x_{i,j} \quad \text{and} \quad b_i = \sum_{j \in \mathcal{B}_i} x_{i,j} \tag{3.5}$$

We want the imbalance imb_i to reflect the time difference between front and back processing times at each stop. Therefore, we define the imbalance as the maximum of the two possible differences.

$$|\tau(f_i - b_i)| = \max\left(f_i - b_i, b_i - f_i\right) \tag{3.6}$$

Thus

$$imb_i \geq \tau\left(f_i - b_i\right) \quad \text{and} \quad imb_i \geq \tau\left(b_i - f_i\right) \tag{3.7}$$

Or equivalently

$$imb_i \geq |\tau(f_i - b_i)| \quad \forall i \in \mathcal{S} \tag{3.8}$$

The objective function is to minimize the total idle time, expressed as follows

$$\min \sum_{i=1}^{S} imb_i \tag{3.9}$$

Given the constraints and objective function, we can formulate the optimization problem as follows:

$$\begin{aligned} \text{minimize} \quad & \sum_{i=1}^{S} imb_i \\ \text{subject to} \quad & \sum_{i=1}^{S} x_{i,j} = 1 \quad \forall j \in \mathcal{T} \\ & x_{i,j} = 0 \quad \text{if} \quad j \notin \mathcal{V}_i \end{aligned} \tag{3.10}$$

An advantage of an optimization-based approach is that once the problem is formulated we can use existing optimization libraries to obtain the solution. In our case, we used the `Google OR-Tools`[1] library to solve our combinatorial problem.

The pipeline for the optimization-based approach is as follows:

1. Compute **candidate stops** based on the robot's current position and weed detections.

1 OR-Tools is an open source software suite for optimization, tuned for tackling the world's toughest problems in vehicle routing, flows, integer, linear, and constraint programming. https://developers.google.com/optimization

2. **Associate** reachable weeds with candidate stops.
3. Build the **optimization model** using decision variables, constraints, and objective function.
4. **Call solver** to get solution.
5. **Decode solution** and return the next optimal stop and task allocation as the algorithm's output.

This method does not suffer from high processing times as weed density increases. The algorithm consistently returns a solution in less than 0.1 seconds across a range of weed densities, from low to extremely high (tested up to 6.25 weeds/m²), making it a strong candidate for real-time applications. The optimization model effectively balances tasks between tools while minimizing idle time. Figure 3.10 illustrates an example of the solution generated by the optimization algorithm in a scenario with twenty weeds.

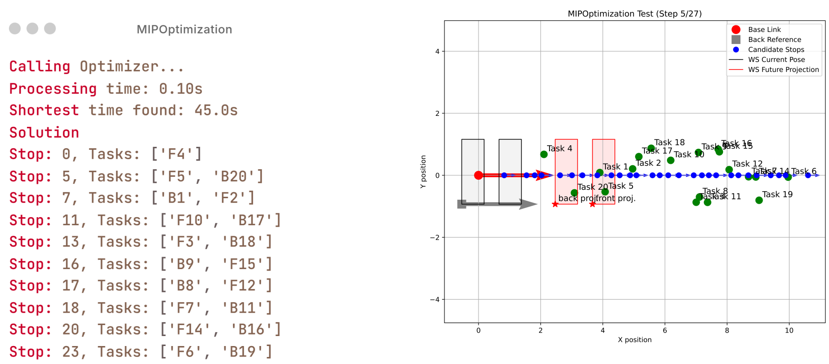

(a) Optimization Output (b) Task Planning Visualization

Figure 3.10: Mixed-Integer Programming Solution

3.5 MARKET-BASED

Market-based approaches are a class of algorithms that leverage the principles of supply and demand to solve task allocation problems. In our context, we consider the set of visible tasks from each candidate stop ($\mathcal{V}_i \subseteq \mathcal{T}$). Given these tasks, the algorithm forms all possible combinations of allocations and generates a bid for each one. The allocation is then determined based on the bids received and selecting the best one. A *'better bid'* is defined as the combination that maximizes the number of removed weeds while minimizing the imbalance between tools (i.e., idle time). The algorithm is designed to be fast and efficient, making it suitable for real-time applications. Nevertheless, since the approach always selects the best next stop, it falls into the category of greedy algorithms due to its shortsighted nature. In some cases, it is necessary to sacrifice productivity at the next stop to benefit the overall solution, as illustrated in Figure 3.4 and Figure 3.5. The main advantage of this approach is its ability to adapt to dynamic environments where tasks change over time.

The next stop computation follows a similar pipeline to previous algorithms, with the main differences being the use of a bidding process to determine the best solution and the computation of candidate stops. Algorithm 2 outlines the steps involved during the algorithm.

Algorithm 2 Run Algorithm (Market-Based)

Require: Current tasks and robot pose
Ensure: Best stop and task assignment with shortest idle time

```
candidate_stops ← get_candidate_stops()
associate_tasks_with_stops(candidate_stops)
if log_print then
  log("Collecting Biddings...")
end if
start_timer()
(stop, tasks, idle_time) ← get_best_bid()
sw_time ← stop_timer()
if log_print then
  log("Processing time: " sw_time"s")
  log("Shortest time found: " idle_time"s")
end if
return (stop, tasks, idle_time)
```

The candidate stops are computed by considering only the closest weed detection and the events this task generate within the back tool workspace. These events include:

1. Entering the workspace.
2. The stop position where the weed is about to exit (rather than when it fully exits).

Using these two candidate poses, we generate evenly distributed positions to create additional candidates between these two events. Afterwards, we perform task association per stop as usual and call `get_best_bid` to start the bidding process and obtain the solution. The algorithm iterates through all possible combinations of tasks at each stop, calculating the idle time for each combination. The combination with the lowest idle time and more number of weeds is selected as the best bid. This process is repeated for all candidate stops, and the best overall stop and task allocation are returned (observe Algorithm 3).

Algorithm 3 Get Best Bid

Require: Candidate stops with associated tasks
Ensure: Best stop and task assignment with minimum idle time

```
bid ← Bid(∅, ∞)
stops ← [ ]
best_stop ← None
best_bid ← None
for i, stop ∈ enumerate(candidate_stops) do
    tasks_per_stop ← [ ]
    for task ∈ stop["tasks"] do
        tasks_per_stop.append(task)
    end for
    combinations ← get_all_combinations(tasks_per_stop)
    idle ← get_idle_per_combination(combinations)
    bid ← get_bid(zip(combinations, idle))
    if update_bid_if_better(bid) then
        best_stop ← i
        best_bid ← bid
    end if
end for
return stops[best_stop], best_bid.tasks, best_bid.idle
```

An example of the solution produced by this algorithm is illustrated in Figure 3.11. We can observe that only four candidate stops are generated for four tasks. Notice the contrast with the graph search in Figure 3.8b and the optimization approach in Figure 3.10b.

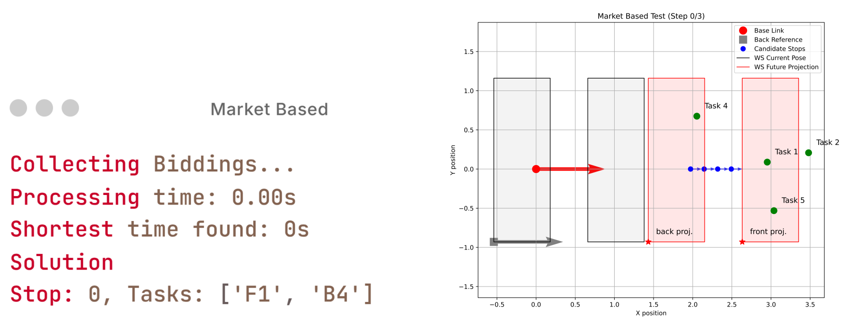

(a) Market-based Output (b) Task Planning Visualization

Figure 3.11: Market-based Solution

4

RESULTS

This chapter presents the simulation results and a comparison between all proposed methods in different scenarios variating from low to high weed density infestation. The goal of this chapter is to come up with the best solution for the task allocation problem and measure the performance improvement over the baseline method.

Paltech currently offers its weeding solutions in fields ranging from 0.5 to 20 hectares, with an average weed density of 0.4 to 1.0 weeds/m^2. Figure 4.1a shows an example of usual weed density in a 1-hectare field, while Figure 4.1b illustrates the coverage path planning pattern that the robot follows in the same field. The simulations in this thesis are limited to the linear movements shown in 4.1b, due to the motion constraints described at the beginning of chapter 3. As a result, the simulation environments were designed accordingly.

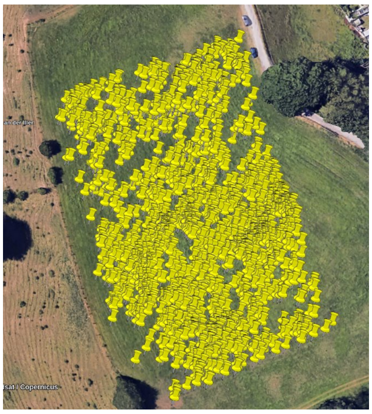

(a) Weed density

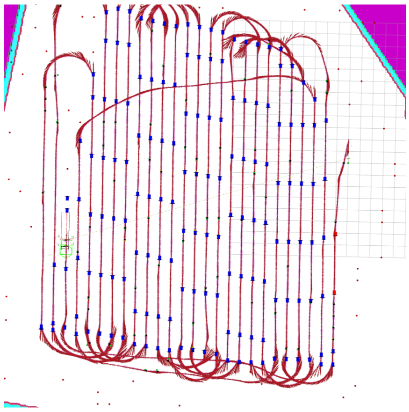

(b) Coverage path planning pattern

Figure 4.1: Weed distribution and coverage path in an agricultural field

4.1 SIMULATION SETUP

Simulations were customized using YAML files, as mentioned in Section 2.2, allowing for ease of configuration and logging convenience. All tests took place in a rectangular grass field of 10m × 50m, with different weed densities along a straight strip of 2m × 50m, simulating one line of the coverage path planning (observe an example in Figure 4.2). The local weed distribution within each quadrant (2m × 2m) varied in both type (*uniform* or *clustered*) and density, replicating irregular Rumex growth.

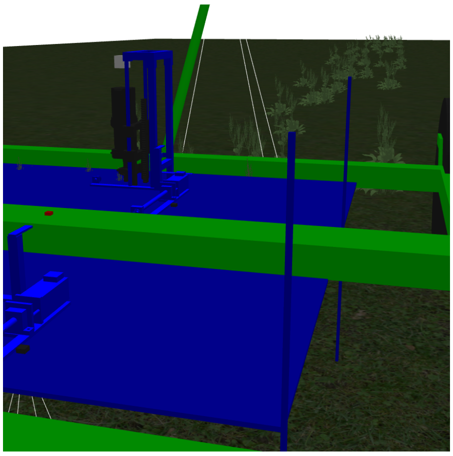

Figure 4.2: Simulation Example

4.2 ALGORITHM COMPARISON

The first simulation corresponds to an infestation area of 100m^2, with a weed density of 0.28 weeds/m^2. This simulates a low weed density scenario, as shown in Figure 4.3a. Figure 4.3 presents both the task visualization and the mission metrics comparison across algorithms.

The first two missions in Figure 4.3b represent the baseline method using one and two tools, respectively. This comparison was made only to determine the natural improvement in mission time when adding an additional tool, even with a non-optimized algorithm. Missions three, four, and five correspond to the graph search, optimization, and market-based approaches, respectively. We observe similar mission times and no significant improvement over the baseline method, which is expected since the weed density is low and, most of the time, the separation between weeds prevents the robot from reaching them with both tools simultaneously. Nevertheless, we observe a reduction in tool idle time with algorithms three, four, and five. The heuristic algorithm results in an idle time of 12.8 min. for the front tool, whereas the others remain within the range of 8 min. to 9.8 min.

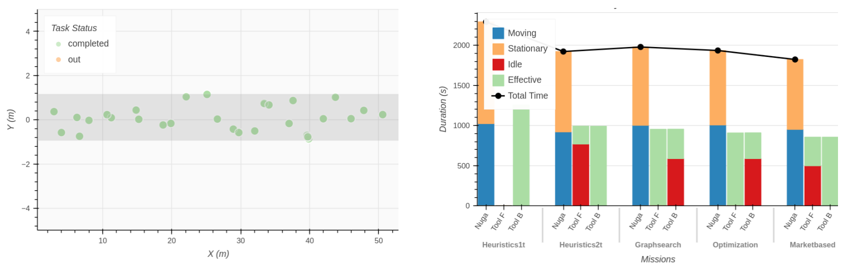

(a) Task Visualization (b) Mission Metrics

Figure 4.3: Low density algorithms comparison

For the second simulation, we increased the average weed density to 0.55 weeds/m^2, simulating a medium-density scenario, as shown in Figure 4.4a. In Figure 4.4b, we observe improvements in both mission time and tool productivity. Both the graph search and optimization-based algorithms show improvements compared to the heuristic approach. Specifically, while the baseline method overuses the back tool, resulting in high idle time for the front tool, graph search and optimization achieve more balanced tool usage. The market-based algorithm also reduces idle time, although not as significantly as the other two methods.

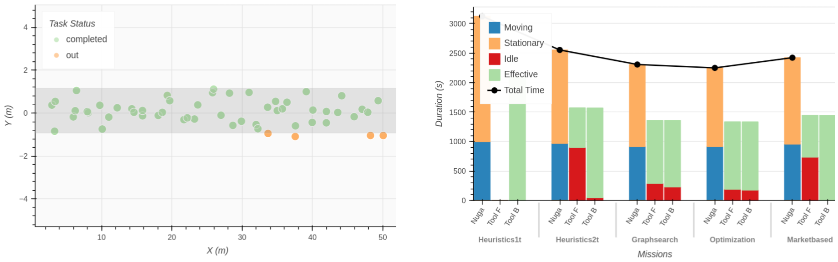

(a) Task Visualization (b) Mission Metrics

Figure 4.4: Medium density algorithms comparison

The third simulation corresponds to a weed density of 1.55 weeds/m^2, simulating a high-density scenario, as shown in Figure 4.5a. Similar to the medium-density scenario (but more pronounced) the graph search and optimization-based approaches show better performance by reducing both mission time and idle time for both tools, achieving balanced tool usage. The market-based algorithm also shows noticeable improvements, achieving better tool productivity and mission time reduction than the baseline, although it still lags behind the other two methods.

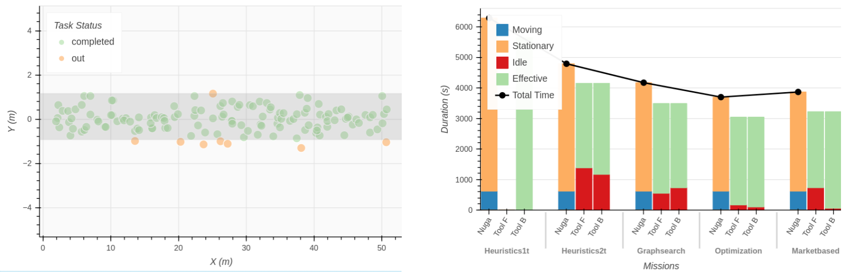

(a) Task Visualization (b) Mission Metrics

Figure 4.5: High density algorithms comparison

The simulation results are summarized in Table 4.1, Table 4.2, Table 4.3 for the low, medium, and high-density simulations, respectively. Each table presents the same information as the previous bar graphs under the '*Raw*' column. Additionally, the '*Improvement*' column shows the relative percentage difference of each algorithm compared to the baseline method for each category. This allows to determine the best algorithm for each weed density scenario.

		Raw (min)					Improvement (%)				
		Mov.	Stat.	Total	Idle	Eff.	Mov.	Stat.	Total	Idle	Eff.
Heuristics	N	15.3	16.7	32	-	-	-	-	-	-	-
	FT	-	-	-	12.8	3.7	-	-	-	-	-
	BT	-	-	-	0.1	16.4	-	-	-	-	-
Graph Search	N	16.7	16.2	32.9	-	-	9.2	-3.0	2.8	-	-
	FT	-	-	-	0.1	15.7	-	-	-	-99.2	324.3
	BT	-	-	-	9.8	6.1	-	-	-	9700.0	-62.8
Optimization	N	16.7	15.4	32.2	-	-	9.2	-7.8	0.6	-	-
	FT	-	-	-	0.1	14.9	-	-	-	-99.2	302.7
	BT	-	-	-	9.8	5.3	-	-	-	9700.0	-67.7
Market	N	15.8	14.5	30.3	-	-	3.3	-13.2	-5.3	-	-
	FT	-	-	-	8.3	5.9	-	-	-	-35.2	59.5
	BT	-	-	-	0.1	14.2	-	-	-	0.0	-13.4

Table 4.1: Low-density Simulation Results

TABLE 4.1 Illustrates the convention used to represent the graph.

		Raw (min)					Improvement (%)				
		Mov.	Stat.	Total	Idle	Eff.	Mov.	Stat.	Total	Idle	Eff.
Heuristics	N	16.1	26.4	42.5	-	-	-	-	-	-	-
	FT	-	-	-	15	11.1	-	-	-	-	-
	BT	-	-	-	0.7	25.3	-	-	-	-	-
Graph Search	N	15.2	23.1	38.4	-	-	-5.6	-12.5	-9.6	-	-
	FT	-	-	-	4.8	17.8	-	-	-	-68.0	60.4
	BT	-	-	-	3.8	18.8	-	-	-	442.9	-25.7
Optimization	N	16	24.5	40.6	-	-	-0.6	-7.2	-4.5	-	-
	FT	-	-	-	1.7	22.4	-	-	-	-88.7	101.8
	BT	-	-	-	9.8	14.2	-	-	-	1300.0	-43.9
Market	N	15.9	24.4	40.3	-	-	-1.2	-7.6	-5.2	-	-
	FT	-	-	-	12.2	11.8	-	-	-	-18.7	6.3
	BT	-	-	-	0	24	-	-	-	-100.0	-5.1

Table 4.2: Medium-density Simulation Results

		Raw (min)					Improvement (%)				
		Mov.	Stat.	Total	Idle	Eff.	Mov.	Stat.	Total	Idle	Eff.
Heuristics	N	10.3	69.4	79.8	-	-	-	-	-	-	-
	FT	-	-	-	23	46	-	-	-	-	-
	BT	-	-	-	19.5	49.6	-	-	-	-	-
Graph Search	N	10.3	59.1	69.4	-	-	0.0	-14.8	-13.0	-	-
	FT	-	-	-	9.1	48.9	-	-	-	-60.4	6.3
	BT	-	-	-	12.1	45.9	-	-	-	-37.9	-7.5
Optimization	N	10.3	51.2	61.6	-	-	0.0	-26.2	-22.8	-	-
	FT	-	-	-	2.8	47.8	-	-	-	-87.8	3.9
	BT	-	-	-	1.7	48.9	-	-	-	-91.3	-1.4
Market	N	10.3	54	64.4	-	-	0.0	-22.2	-19.3	-	-
	FT	-	-	-	12.2	41.4	-	-	-	-47.0	-10.0
	BT	-	-	-	1	52.6	-	-	-	-94.9	6.0

Table 4.3: High-density Simulation Results

Part I

APPENDIX

You can put some informational part preamble text here. Illo principalmente su nos. Non message *occidental* anglo-romanic da. Debitas effortio simplificate sia se, auxiliar summarios da que, se avantiate publicationes via. Pan in terra summarios, capital interlingua se que. Al via multo esser specimen, campo responder que da. Le usate medical addresses pro, europa origine sanctificate nos se.

A

APPENDIX TEST

Lorem ipsum at nusquam appellantur his, ut eos erant homero concludaturque. Albucius appellantur deterruisset id eam, vivendum partiendo dissentiet ei ius. Vis melius facilisis ea, sea id convenire referrentur, takimata adolescens ex duo. Ei harum argumentum per. Eam vidit exerci appetere ad, ut vel zzril intellegam interpretaris.

More dummy text.

A.1 CONFIGURATION FILES

YAML files are the standard method for setting up configuration variables in the Nuga project. A collection of configuration examples is provided in this appendix.

Listing A.1: Weed Infestation World config example

```yaml
seed: 2
quadrant_size: [2.0, 2.0]
quadrants:
  1:
    direction: x
    weed_density: 0.4   # weeds/m2
    spatial_distribution: clustered
    std_dev: [0.5, 0.5]
    outside_workspace: false

  2:
    direction: x
    weed_density: 1.2   # weeds/m2
    spatial_distribution: uniform
    outside_workspace: false
```

Listing A.2: ROS2 config example

```yaml
# ROS2 Control
controller_manager:
  ros__parameters:
    use_sim_time: True
    update_rate: 20 # Hz

    joint_state_broadcaster:
      type: joint_state_broadcaster/JointStateBroadcaster

    forward_position_controller_front:
      type: forward_command_controller/ForwardCommandController

    forward_position_controller_back:
      type: forward_command_controller/ForwardCommandController

forward_position_controller_front:
  ros__parameters:
    joints:
      - front_x_axis_joint
      - front_y_axis_joint
      - front_implement_tool_joint
    interface_name: position

forward_position_controller_back:
  ros__parameters:
    joints:
      - back_x_axis_joint
      - back_y_axis_joint
      - back_implement_tool_joint
    interface_name: position
```

A.2 ALGORITHMS

Algorithm 4 Depth-First Search

Require: *root_node*, *last_node*
Ensure: Explored Graph

```
visited ← {last_node} {Initialize with last node}
stack ← [root_node] {Start with root node}
i ← 0 {Iteration counter}
while stack is not empty do
    i ← i + 1
    node ← stack.pop()
    if node ∉ visited then
        visited.add(node)
        children ← get_children_nodes(node)
        if children ≠ None then
            stack.extend(children) {Add children to stack}
        end if
    end if
    if i == 5000 then
        break {Early termination}
    end if
end while
```

Algorithm 5 Dijkstra's Algorithm

Require: *graph*, *start_node*, *goal_node*
Ensure: Shortest path from *start_node* to *goal_node*

$cost \leftarrow$ defaultcost(∞) {Distance from start to each node}
$prev \leftarrow$ dict() {To reconstruct shortest path}
$cost[start\_node] \leftarrow 0$
$queue \leftarrow$ priority queue initialized with $(0, start\_node)$
while queue is not empty **do**
  $(current\_cost, current\_node) \leftarrow$ queue.pop()
  if $current\_node == goal\_node$ **then**
    break
  end if
  for all *neighbor* of *current_node* in *graph* **do**
    $new\_cost \leftarrow current\_cost +$ weight$(current_node, neighbor)$
    if $new\_cost < cost[neighbor]$ **then**
      $cost[neighbor] \leftarrow new\_cost$
      $prev[neighbor] \leftarrow current\_node$
      queue.push$(new_cost, neighbor)$
    end if
  end for
end while
return shortest path and cost from *start_node* to *goal_node*

A.3 ANOTHER APPENDIX SECTION TEST

Equidem detraxit cu nam, vix eu delenit periculis. Eos ut vero constituto, no vidit propriae complectitur sea. Diceret nonummy in has, no qui eligendi recteque consetetur. Mel eu dictas suscipiantur, et sed placerat oporteat. At ipsum electram mei, ad aeque atomorum mea. There is also a useless Pascal listing below: Listing A.3.

Listing A.3: A floating example (`listings` manual)

```
for i:=maxint downto 0 do
begin
{ do nothing }
end;
```

[1] Xinye Chen, Ping Zhang, Fang Li, and Guanglong Du. "A cluster first strategy for distributed multi-robot task allocation problem with time constraints." In: *2018 WRC Symposium on Advanced Robotics and Automation (WRC SARA)*. 2018, pp. 102–107. DOI: 10.1109/WRC-SARA.2018.8584210.

[2] Ahmed Elfakharany and Zool Hilmi Ismail. "End-to-End Deep Reinforcement Learning for Decentralized Task Allocation and Navigation for a Multi-Robot System." In: *Applied Sciences* 11.7 (2021). ISSN: 2076-3417. DOI: 10.3390/app11072895. URL: https://www.mdpi.com/2076-3417/11/7/2895.

[3] Junyan Hu, Parijat Bhowmick, Inmo Jang, Farshad Arvin, and Alexander Lanzon. "A Decentralized Cluster Formation Containment Framework for Multirobot Systems." In: *IEEE Transactions on Robotics* 37.6 (2021), pp. 1936–1955. DOI: 10.1109/TRO.2021.3071615.

[4] Athira K A, Divya Udayan J, and Umashankar Subramaniam. "A Systematic Literature Review on Multi-Robot Task Allocation." In: *ACM Comput. Surv.* 57.3 (Nov. 2024). ISSN: 0360-0300. DOI: 10.1145/3700591. URL: https://doi.org/10.1145/3700591.

[5] Jeongeun Kim and Hyoung Il Son. "A Voronoi Diagram-Based Workspace Partition for Weak Cooperation of Multi-Robot System in Orchard." In: *IEEE Access* 8 (2020), pp. 20676–20686. DOI: 10.1109/ACCESS.2020.2969449.

[6] Donald E. Knuth. "Computer Programming as an Art." In: *Communications of the ACM* 17.12 (1974), pp. 667–673.

[7] Jiamei Lin, Pengcheng Li, Jialong Dai, Shaorui Liu, Wei Tian, Bo Li, and Changrui Wang. "Multi-robot Cooperative Assembly Task Planning for Large-scale Aerospace Structures." In: *2022 37th Youth Academic Annual Conference of Chinese Association of Automation (YAC)*. 2022, pp. 795–800. DOI: 10.1109/YAC57282.2022.10023897.

[8] Nicholas Lindsay, Robert K. Buehling, and Lihong Sun. "A Sequential Task Addition Distributed Assignment Algorithm for Multi-Robot Systems." In: *Journal of Intelligent & Robotic Systems* 102 (2021), p. 51. DOI: 10.1007/s10846-021-01394-7.

[9] Xingjie Liu, Guolei Wang, and Ken Chen. "Option-Based Multi-Agent Reinforcement Learning for Painting With Multiple Large-Sized Robots." In: *IEEE Transactions on Intelligent Transportation Systems* 23.9 (2022), pp. 15707–15715. DOI: 10.1109/TITS.2022.3145375.

[10] Javier G. Martin, Francisco Javier Muros, José María Maestre, and Eduardo F. Camacho. "Multi-robot task allocation clustering based on game theory." In: *Robotics and Autonomous Systems* 161 (2023), p. 104314. ISSN: 0921-8890. DOI: https://doi.org/10.1016/j.robot.2022.104314. URL: https://www.sciencedirect.com/science/article/pii/S0921889022002032.

[11] R. J. Panciera, T. Martin, G. E. Burrows, D. S. Taylor, and L. E. Rice. "Acute oxalate poisoning attributable to ingestion of curly dock (Rumex crispus) in sheep." In: *Journal of the American Veterinary Medical Association* 196.12 (1990), pp. 1981–1984.

[12] Darren Smith, Jodie Wetherall, Stephen Woodhead, and Andrew Adekunle. "A Cluster-Based Approach to Consensus Based Distributed Task Allocation." In: *2014 22nd Euromicro International Conference on Parallel, Distributed, and Network-Based Processing*. 2014, pp. 428–431. DOI: 10.1109/PDP.2014.87.

[13] Shiguang Wu, Xiaojie Liu, Xingwei Wang, Xiaolin Zhou, and Mingyang Sun. "Multi-robot Dynamic Task Allocation Based on Improved Auction Algorithm." In: *2021 6th International Conference on Automation, Control and Robotics Engineering (CACRE)*. 2021, pp. 57–61. DOI: 10.1109/CACRE52464.2021.9501305.

[14] T. Zhang, Q. Li, Cs. Zhang, et al. "Current trends in the development of intelligent unmanned autonomous systems." In: *Frontiers in Information Technology & Electronic Engineering* 18 (2017), pp. 68–85. DOI: 10.1631/FITEE.1601650.

DECLARATION

Put your declaration here.

Zagreb, Croatia, June 2025

David Razhiel Ceres Arroyo

COLOPHON

This document was typeset using the typographical look-and-feel `classicthesis` developed by André Miede and Ivo Pletikosić. The style was inspired by Robert Bringhurst's seminal book on typography "*The Elements of Typographic Style*". `classicthesis` is available for both LaTeX and LyX:

https://bitbucket.org/amiede/classicthesis/

Happy users of `classicthesis` usually send a real postcard to the author, a collection of postcards received so far is featured here:

http://postcards.miede.de/

Thank you very much for your feedback and contribution.